International Journal of Pharmaceutical Research and Applications
Volume 9, Issue 2 Mar-Apr 2024, pp: 273-282 www.ijprajournal.com ISSN: 2249-7781

Gait Analysis and Locomotion Control Using Wearable Sensors and Actuators through IOT

Samir Sharma[1],Atreyee Sharma[2], Utpal Kumar Paul[3], Amar Prakash Sinha[4.]
[1, 3, 4] *Dept. of ECE, BIT Sindri, Jharkhand, India, PIN: 828123.*
[2]*Dept. of Physiotherapy, MMDU, Mullana, Ambala, India. PIN: 133207.*

Submitted: 11-03-2024 Accepted: 21-03-2024

ABSTRACT: Analysis of gait using wearable sensors is a low-cost, but efficient way of diagnosing gait problems. The involvement of actuators as a clinical tool in the process of rehabilitation shows great prospects. Thispaper presentsa model ofgait analysis and optimization of locomotion using wearable Sensors and actuators through IOT. The gait analysis methods based on wearable sensors areprimarily divided into gait kinematics, gait kinetics, and electromyography. Applications of the concept in sports, rehabilitation, and clinical diagnosis are modeled separately. With the development of customizedsensors gait analysis using wearable sensors has opened multiple directions of gait control in clinical applications.The development of dedicated controllers for powered prostheses is a daunting task that requires involvement from clinicians, patients, and robotics experts.The proposed device is lighter and targeted for various typesof handicaps. These could be the loss of stamina because of aging, the loss of strength, loss of coordination because of spinal cord injury (SCI), neurodegenerative diseases, and even loss of limbs.

KEYWORDS: Gait analysis; Wearable sensors; Robotic prosthetic lower limbs;PID/fuzzy logic controller.

I. INTRODUCTION

In recent times wearable sensors for gait measurement and analysis gained huge improvements in feasibility and application. These systems use inertial measurement sensors such as gyroscopes, accelerometers, and magnetometers for measuring the motion of limb segments and body parts (Modar Hassan, 2014) [1]. Through gait analysis, the gait phases can be identified and the kinetic parameters of human gait events can be determined, and musculoskeletal functions can be quantitatively evaluated. After detection of quantized gait information assisted movement of limbs can be generated using optimization techniques like ant colony optimization. Multi-camera motion capture systems have been widely used for standard gait analysisfor long. The use of customised sensors can provide data like angle of movement, distance,etc. which can further be used to diagnosethe problem.

People with gait movement problems can be assisted with automatically activated actuators.Currently, Conventional Knee Orthosis (CKO) devicesare verycommonly used because of their simple structure and low cost. A CKO device assists a user in maintainingstance stability and free knee swing while changing position. However,a CKO device has its limitations and cannot enable a user to have anatural gait.An activeKnee Orthosis (AKO) device has been developed to help a user have natural gait movement. An AKO device usually combines a knee orthosis frame with an active actuator, sensors, and a controller (Shiao, 2017)[2].

With a well-designed control algorithm of optimization, an AKO device can enable a user to walk more naturally but with optimum velocity and balance. Adaptive knee orthosis can be designed with an electric motor. However, an AKO device usually suffers from heavy mass, high power consumption, complex structure, and high cost. Therefore, the uses of AKO devices are mostly used for persons with extreme disabilities (Beyl, 2007)[3].

Individuals with lower limb loss or non-responding are restricted in their mobility with a reduction in physical movement. Passive prosthetic legs are also not capable of providing the net positive work required for many daily tasks. Emerging powered prostheses have thepotential to address this limitation through the use of jointactuators and sensors. However,the significantincrease in device weight and costis still a constraint.To address these limitations in amputee locomotion, robotic prosthetic lower limbs are being developed with the desired specifications for achieving at-par movement of able-bodied human

beings (Emma Reznick, 2021)[4]. The proposed model not only attempts to improve the limitation but also optimizes the different parameters like velocity, balance, and power.
The health care professional can monitor, supervise, and monitor the parameters as set by the optimizer through IOT technology.

II. PROPOSED MODEL

The proposed model consists of 8 motors as shown in table I. The proposed location of the left-side motors is shown in Figure 1.

TABLE I

(Motors to replicate lower limbs)

Sl. No.	Motor	Location	Function
1	M_{HL}	Left side of HIP	To rotate the left femur
2	M_{HR}	Right side of HIP	To rotate the right femur
3	M_{KL}	Knee of left leg	To rotate the left tibia and sibula
4	M_{KR}	Knee of right leg	To rotate the left tibia and sibula
5	M_{AL}	Ankle of left leg	To rotate the left foot complex
6	M_{AR}	Ankle of right leg	To rotate the right foot complex
7	M_{TL}	Toe of left leg	To rotate the left toe
8	M_{TR}	Toe of right leg	To rotate the right toe

The proposed model classifies the seven different loco motions walking, running, ascending, and descending. An able-bodied experiment was conducted to obtain the desired data through a wearable sensing method (Emily G. Keller, 2022)[5]. Thedata for these eight motors and for such locomotion are collected fromable-bodied persons. The data for all these motions are stored in a data bank. Now, the data for the desired motion is fed to the Micro Controller Unit (MCU)/Fuzzy Controller Unit(FCU) which drives the powered robotic prosthetic lower limbs. When the disabled person is asked to perform that action or wishes to do that by himself or herself, the MCU/FCU will guide, control, and optimize the motion of the limb. The MCU is fed with primary data from the data bank. At a later stage to provide stability, the primary data is updated by stochastic optimization and healthcare professionals from a remote end.Here, a standard stochastic optimization framework has been used to optimize the power consumption of the powered devices, the angular velocity of the motor, the torque applied to the motors, etc. For the sake of simplicity, data for walking only has been mentioned here.

Figure 1: Walking on a treadmill

An able-bodied individual was asked to walk on a treadmill and photos were shot to measure all the parameters of all thephases of walking**(Weijun Tao, 2012)**[6].

Heel Strike: This phase starts at the moment when the heel first touches the ground and lasts until the whole foot is on the ground known as the early flatfoot stage.

Early flatfoot: Then the next phase begins as soon as the moment that the whole foot is on the ground. It ends with the body's center of gravity (normally located approximately in the pelvic area in front of the lower spine) passing over the top of the foot.

Late flatfoot: Once the body's center of gravity has passed through the pelvic area, the "late flatfoot" stage begins and ends when the heel lifts off the ground.

Heel rise: The heel rise phase begins when the heel begins to leave the ground.

Toe-off**:** The toe-off stage of gait begins as the toes leave the ground. This represents the start of the swing phase.

A data table as a partial result is attached here.Optimization of the power consumption is one of the keysto the success of the model. Photovoltaic power has been used to provide power for the modified direct torque-controlled (DTC) induction motor (Naveen Goel, 2020)[7].

TABLE II
(Maximum Angle of the Junction)

Motion	Junction Involved	Maximum angle
Walking	Hip (α_H)	-18^0 to 28^0
	Knee (α_K)	-2^0 to 48^0
	Ankle (α_A)	-25^0 to 8^0
	Toe (α_T)	0^0 to 80^0

TABLE III
(Rangege Angular Velocity)

Motion	Junction Involved	Range of Angular Velocity in (rad/Sec)	
		Highest	Lowest
Walking	Hip	1.2	1.0
	Knee	0.7	0.6
	Ankle	0.7	2.1
	Toe	Not measured	

The overall operation of the proposed model has been described the the flowchart in Figure 2. Each joint has been replicated by a series of geared BLDC motors to obtain the desired degree of freedom. For the simplicity of representation, only one degree of freedom has been developed.

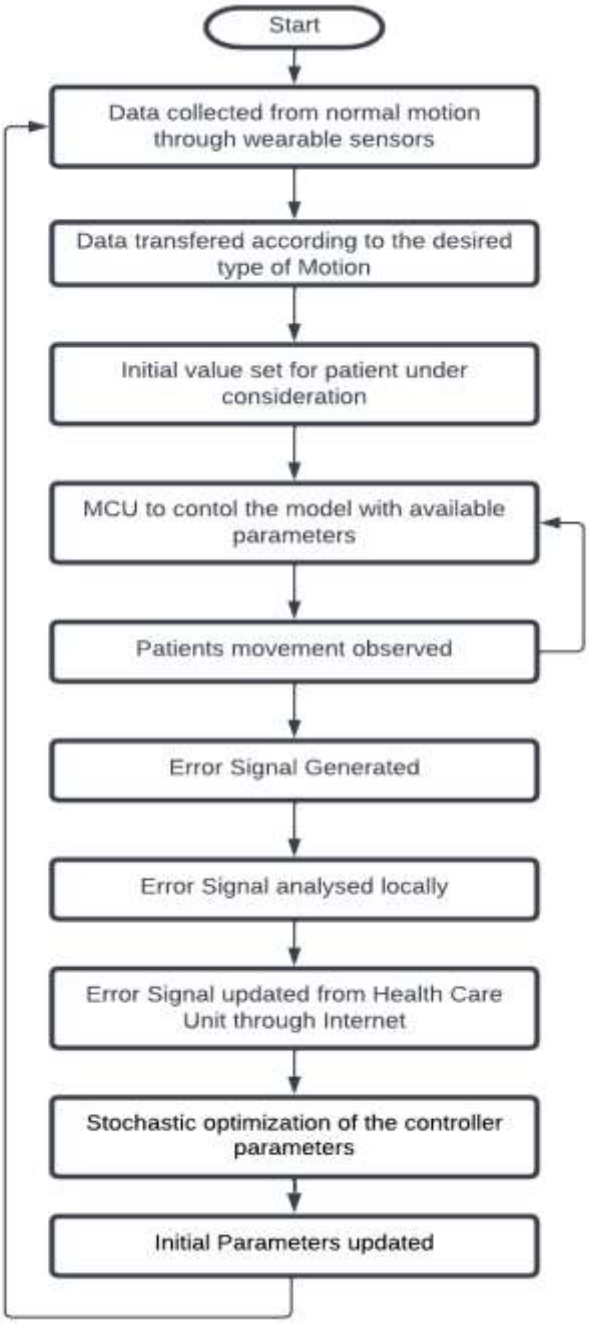

Figure 2: Proposed model in flowchart

Thus, the proposed model can be described through the block diagram as shown in Figure 3. Here the central MCU (ATmega 328) and connected through Wi-Fi (ESP8266) were used to control the speed from a remote location. For the purpose of selection of DC Motor and analysis of performance the Simulink model has been used.

International Journal of Pharmaceutical Research and Applications
Volume 9, Issue 2 Mar-Apr 2024, pp: 273-282 www.ijprajournal.com ISSN: 2249-7781

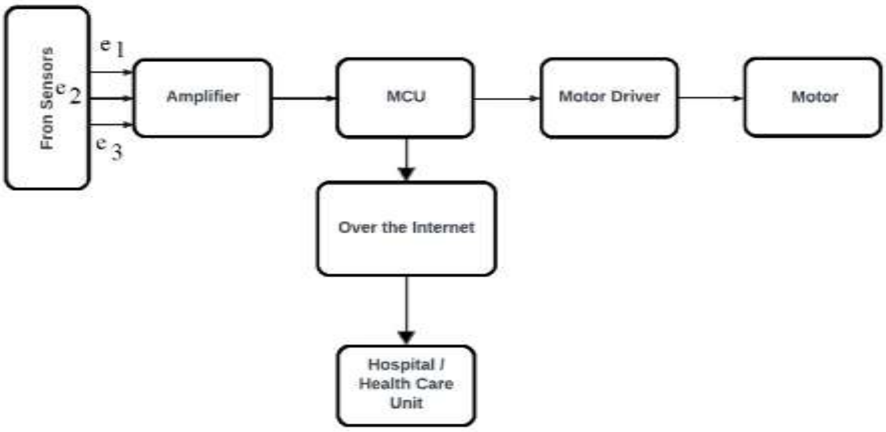

III. ANALYSIS OF MOVEMENT

Electromyography (EMG) is an electrodiagnostic technique for evaluating and recording the electrical activity produced by skeletal muscles (Ching-Kun Chen, 2020)[8].Different Researchers recorded lower-limb kinematics and Electromyogram(EMG) of able-bodied participants during free transitions between sitting, standing, level-ground walking, ramp walking, running, and stair climbing (Hu B, 2018)[9]. Neuromechanical signals were recorded from these able-bodied individuals using wearable sensors during unassisted locomotion. A general classification of all these locomotion (as indicated by M1 to M7) is shown in Figure

3.In the proposed model the base position has been considered as standing mode. The algorithm for all movements begins from this mode only. For any of the following motions, there is at least one joint to work. Therefore, analysis of only one junction out of eightand one movement out of seven have been analyzed and optimized here.

Electromagnetic motors with gears with features like lightweight, high torque/weight ratio, and high torque control performance are of primary requirement for the achievement of the desired movement of all the junctions under consideration (Daichi Kondo, 2021)[10].

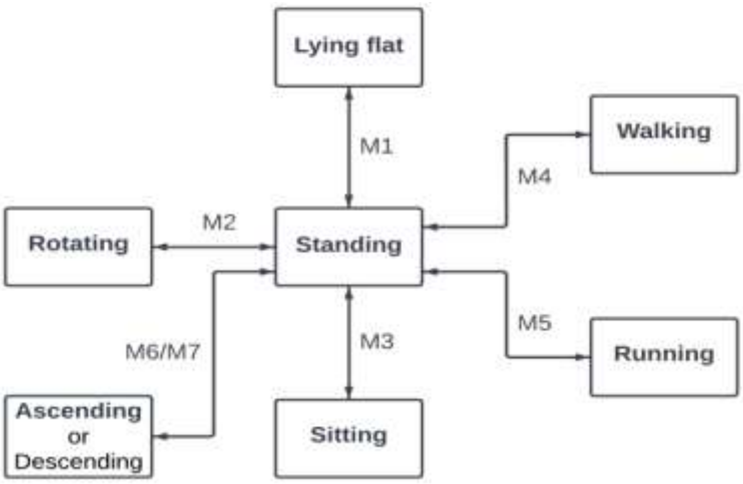

FIGURE 3: LOCOMOTION MODES AND PRACTICAL MOVEMENTS (M1 THROUGH M7)

International Journal of Pharmaceutical Research and Applications
Volume 9, Issue 2 Mar-Apr 2024, pp: 273-282 www.ijprajournal.com ISSN: 2249-7781

Sitting(M3): Data for 'Sit-to-stand'and 'stand-to-sit'transitions were collected by instructing the participant to sit or stand.

Rotating(M2): Transitions for the desired degree in multiple of 5 like 5^0, 10^0, $15^{0,}$ and so on till 180^0 were recorded in both positive and negative directions.

Lying Flat(M1): Participants were asked to lie flat from a standing position and to stand up again.

Walking(M4):Walking trials, progressed through a range of a few meters of nominal walking has been recorded.

Running(M5): Able-bodied participants were again asked to run on the treadmill for a few minutes. Data was collected for a few seconds for running trials in a randomized order of different speeds.

Ascending and descending(M6/M7):Stair(as shown in Figure4) trials were conducted over four inclinations (φ) of stairs (20°; 25°; 30° and 35°). The participantsascended5 - 6 ft from the base of the staircase, approached the stairs at a self-selected speed, ascended the stairs, and walked to the end of the platform. At this point, the capture was ended and the participantswereasked to turnaround (M2). This procedure recorded the motion from A to B and then B to A in Figure 4.Then the participantswereasked todescendthe trial from rest at the end of the platform, descend to the bottom of the stairs, and continue to the demarcated starting line. A sufficient number of ascent and descent trials were conducted.

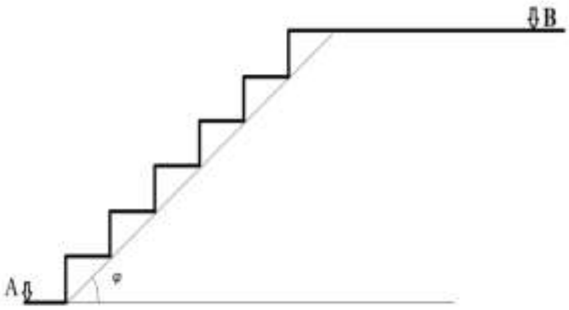

FIGURE 4: STRUCTURE OF STAIRS FOR TRIAL

Initially, athree-dimensional image is formed for each of the above-mentionedmotions. The velocity of each sensor in forward or backward, vertically upward or downward, laterally left or write are recorded to form the degree of freedom for each motor.Some preset values are set based on these data. These parameters would be used as the initial or primary data in Figure5 but can be modified later either by the controller embedded within the powered prostheticlimb or by the health care professional from the remote end through the internet.

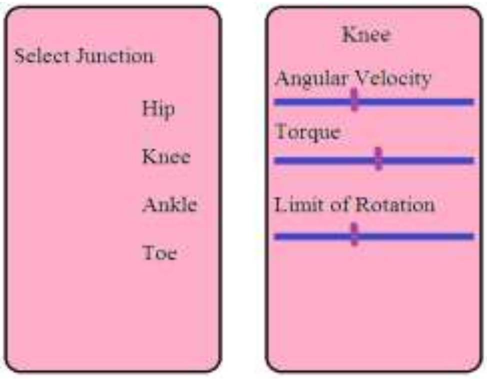

FIGURE 5: PROPOSED LAYOUT OF CONTROL THROUGH MOBILE APP

International Journal of Pharmaceutical Research and Applications
Volume 9, Issue 2 Mar-Apr 2024, pp: 273-282 www.ijprajournal.com ISSN: 2249-7781

IV. PROCESS

Theproposed model may be used for the verification of the controllers by means of a simulated environment, reducing the dependency on experimental evaluation and easing the debugging process during software development. Additionally, the researchers are interested in verifying the functionality of the framework by using it to tune the parameters using a stochastic optimization process that searches for the best set of parameters for a given motion task, represented by a control algorithm. Figure 6 presents the block diagram of the complete process of stochastic optimization of the controller parameters.

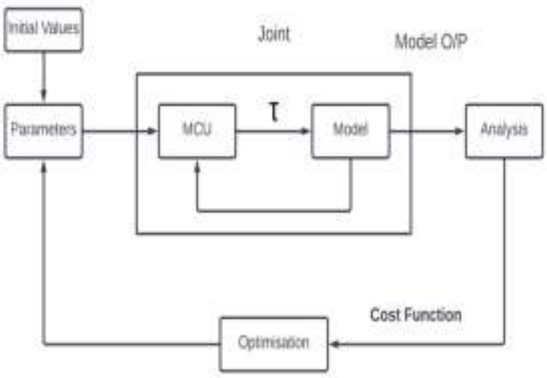

FIGURE 6: OPTIMISATION PROCESS

Using SIMULINK simulations, it can be demonstrated that the fuzzy logic controller achieved more robust and faster control of the speed of the DC motor with zero overshoot. The higher rise and settling time compared with the conventional PID controller justifies its use as the controller (Getu, 2021)[11]. The fuzzy PID controller has been used in its modified form to control the speed of the motor, the load torque was controlled by a Lookup Table prepared from the database as prepared from the trial of able-bodied persons. The stator current, rotor speed, and electromagnetic torque were observed by using the Scope modules of Simulink. The parameters of the PID controller are tuned by the Fuzzy controller according to the real-time system.

The error e(t) and the change of error $\Delta e(t)$ of the angular velocity is the variable inputs of the fuzzy logic controller. The control voltage u(t) is the variable output of the fuzzy logic controller.

$$e(t) = r(t) - u(t)$$

$$\Delta e(t) = e(t) - e(t-1)$$

Using these two minimum inputs a fuzzy controller has been designed through Simulink. Fuzzification, Fuzzy inferencing, and defuzzification were followed here.

Objectives of Optimisation:

The primary objectives of optimization are as follows.

- Minimise power consumption(W), thereby increasing battery life,
- To deliver highest torque(τ),
- To obtain the optimum angular velocity of the junction (α_H, $\alpha_{K,}$ α_A).
- To obtain minimum weight.
- To obtain the highest life.

V. DESIGN

Data obtained from the locomotion of able-bodied persons is the primary result, which is then fed to the proposed controller using both conventional PID controller and fuzzy controller. Then MATLAB/SIMULINK has been used for optimization.

5.1 DESIGN OF THE PROPOSED CONTROLLER

System input: The conventional PID controller has been used as the controller of the brushless DC (BLDC) motor. Figure 7 shows the structure of the conventional PID controller, and the output of a conventional PID controller can be described as the following equation:

$$u(t) = K_p . e(t) + K_i . \int_0^t e(t)dt + K_d . \frac{de(t)}{dt} \text{........(1)}$$

Where u(t) is the output of the PID controller, K_p, K_i, $K_d$are the proportional, integral, and derivative gain, and e(t) is the speed error.

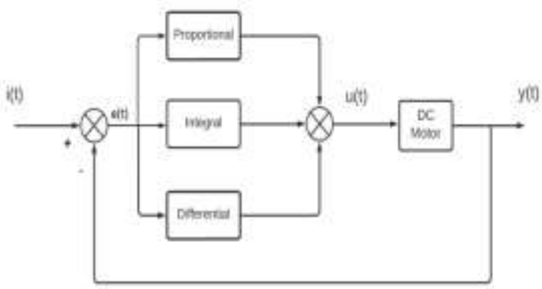

Figure 7: PID Controller

Because of the inherent limitation of continuous PID controller, discrete version of equation (1) is used here.

$$i(k) = K_p . e(k) + K_i . \sum_{j=0}^{k} e(j) + K_d . (e(k) - ek-1..(2)$$

International Journal of Pharmaceutical Research and Applications
Volume 9, Issue 2 Mar-Apr 2024, pp: 273-282 www.ijprajournal.com ISSN: 2249-7781

where e(k), e(k - 1) are the errors at the time of (k) and (k –1).

5.2 SIMULATION MODEL OF MOTOR IN SIMULINK

DC motors are probably the most basic type of electrical motors. In any kind of electric motor, a current-carrying conductor generates a magnetic field;

$V = E_b + I_a R_a$ .... (3)

Where, E_b = back emf in volts,
I_a = armature current in ampere.

If both side of the above equation is multiplied by I_a,

$VI_a = E_b I_a + {I_a}^2 R_a$ .... (4)

Where VI_a = electrical power supplied to the motor,
$E_b I_a$ = electrical equivalent of the mechanical power produced by the motor,
${I_a}^2 R_a$ = power loss taking place in the armature winding,

Equation 4 can be written as

$E_b I_a = VI_a - {I_a}^2 R_a$............ (5)

i.e. Gross mechanical power generated (P_{MG}) by the motor in rpm is

$P_{MG} = E_b I_a$............ (6)

The mechanical power required to rotate the shafton the mechanical side is calculated as

$P_{MR} = \tau\omega$ .... (7)

Where, τ = Torque in Newton.meter
ω = angular velocity in Radian/second

Comparing equation 6 and 7, it can be written

$E_b I_a = \tau\omega$ .... (8)

Therefore,

$\tau = \frac{E_b I_a}{\omega}$ .... (9)

Replacing, ω by 2πN in equation 9, where N is number of rotation per seconnd

$\tau = \frac{E_b I_a}{2\pi N}$ .... (10)

Figure 8 shows the SIMULINK model of motor.

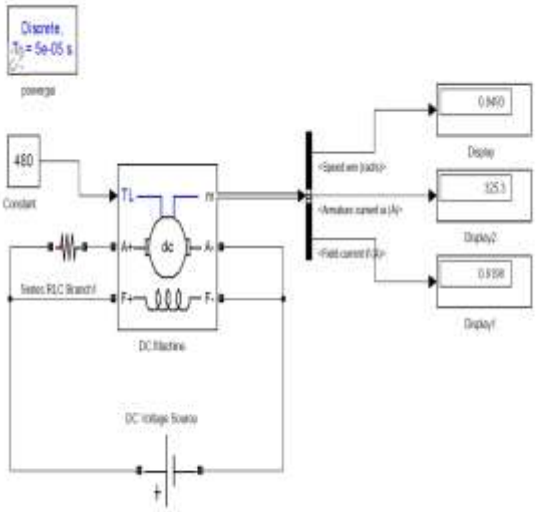

FIGURE 8: SIMULINK MODEL OF DC MOTOR

VI. RESULTS

In the SIMULINK model, desired parameters under variable conditions have been obtained. The speed and torque characteristics of DC motors have been found to be compatible to yield the optimum result. The simulation is conducted on the different operating parameters such as speed, weight of the individual, type of assistance, etc. Some of the results as obtained have been tabulated in TableIV.

TABLE IV
(Motor Performance)

Sl. No	Supply	Type	Parameters	Value
1	120V	Independent	Torque Load (TL) in N.m	178.55
2			Series Resistance in Ω	0.001
4		Dependant	Armature Current (I_a) in A	198.4
5			Speed in rad/s	0.8536
1	48V	Independent	Torque Load (TL) in N.m	28.57
2			Series Resistance in Ω	0.001
4		Dependent	Armature Current (I_a) in A	79.35
5			Speed in rad/s	0.8632

1	24V	Independent	Torque Load (TL) in N.m	7.15
2			Series Resistance in Ω	0.001
4		Dependent	Armature Current (I_a) in A	39.67
5			Speed in rad/s	0.8789

Therefore, it is observed that the Torque load which primarily represents the body weight of the patient can be well managed by changing the DC supply and compensation with speed. This is practically the same when calculated through equation 10. With reference to Table III, angular velocity of the order of 0.6 to 2.1 rad/sec is sufficient enough to rotate any of the three junctions while walking. Table IV clearly depicts that the model can provide the desired Torque at the desired speed and coordination through central MCU, among themselves.

VII. CONCLUSIONS

Power electronic converters are permanently required in DC motors for their electronic commutation for both fixed or variable speed applications. For different purposes, variable speed drives are used in industry. It is the task of the researchers to increase reliability and reduce their overall construction costs.

The result of the experiment through SIMULINK demonstrates that the desired Torque required to move an able-bodied person is achievable. The researchers are in the process of replacing conventional PID controllerswith fuzzy Logic Controller in the field of prosthetic limbs for better optimization.The data that were captured and optimized for better results is ready for trial at different discrete phases of walking and for other locomotion. Once the complete automation with the necessary coordination among all the motors of each joint and with the desired degree of freedom is achieved, the proposed model will be ready for trial. Further progress in producinglightweightmotors will increase the application range of the proposed device.

REFERENCES:

[1]. Hassan M, Kadone H, Suzuki K, Sankai Y. Wearable gait measurement system with an instrumented cane for exoskeleton control. Sensors (Basel). 2014 Jan 17;14(1):1705-22. doi: 10.3390/s140101705. PMID: 24445417; PMCID: PMC3926634.

[2]. Yaojung Shiao, Ting-Yue Chang, and Chien-Hung Lai, Gait Identification by Inertial Sensors for Control of Adaptive Knee Orthosis Device, Sens. Mater., Vol. 29, No. 11, 2017, p. 1657-1665.

[3]. P. Beyl, J. Naudet, R. Van Ham and D. Lefeber, "Mechanical Design of an Active Knee Orthosis for Gait Rehabilitation," 2007 IEEE 10th International Conference on Rehabilitation Robotics, Noordwijk, Netherlands, 2007, pp. 100-105, doi: 10.1109/ICORR.2007.4428413.

[4]. Reznick, E., Embry, K.R., Neuman, R. et al. Lower-limb kinematics and kinetics during continuously varying human locomotion. Sci Data **8**, 282 (2021). https://doi.org/10.1038/s41597-021-01057-9.

[5]. Keller, Emily; Laubscher, Curt; Gregg, Robert (2022). Gait Event Detection with Proprioceptive Force Sensing in a Powered Knee-Ankle Prosthesis: Validation over Walking Speeds and Slopes. TechRxiv. Preprint. https://doi.org/10.36227/techrxiv.21207104.v2

[6]. Tao W, Liu T, Zheng R, Feng H. Gait analysis using wearable sensors. Sensors (Basel). 2012;12(2):2255-83. doi: 10.3390/s120202255. Epub 2012 Feb 16. PMID: 22438763; PMCID: PMC3304165.

[7]. Goel, N., Chacko, S. & Patel, R.N. PI Controller Tuning Based on Stochastic Optimization Technique for Performance Enhancement of DTC Induction Motor Drives. J. Inst. Eng. India Ser. B **101**, 699–706 (2020). https://doi.org/10.1007/s40031-020-00496-z

[8]. Chen, C.-K.; Lin, S.-L.; Wang, T.-C.; Lin, Y.-J.; Wu, C.-L. Lower-Limb Electromyography Signal Analysis of Distinct Muscle Fitness Norms under Graded Exercise Intensity. Electronics **2020**, 9, 2147.

https://doi.org/10.3390/electronics9122147

[9]. Hu B, Rouse E, Hargrove L. Benchmark Datasets for Bilateral Lower-Limb Neuromechanical Signals from Wearable Sensors during Unassisted Locomotion in Able-Bodied Individuals. Front Robot AI. 2018 Feb 19;5:14. doi: 10.3389/frobt.2018.00014. Erratum in: Front Robot AI. 2018 Nov 20;5:127. PMID: 33500901; PMCID: PMC7805660.

[10]. Kondo, Daichi & Yashiro, Daisuke &Yubai, Kazuhiro & Komada, Satoshi. (2021). Load torque control of an electromagnetic motor with a reduction gear and motor/load-side encoders using a spring model including a dead zone. Electrical Engineering in Japan. 214. 10.1002/eej.23360.

[11]. Abdel-Salam, Abdel-Azim. (2022). Comparison between FLC and PID controller for speed control of DC motor. International Robotics & Automation Journal. 8. 40-45. 10.15406/iratj.2022.08.00242.